Journal of JSEM, Vol.9, Special Issue (2009) 162-166

Image-Based Matching for Natural Knee Kinematics Measurement Using Single-Plane Fluoroscopy

Koichi KOBAYASHI[1], Nobuaki TANAKA[2], Ken-ichi ODAGAWA[2], Makoto SAKAMOTO[1] and Yuji TANABE[3]

[1]Department of Health Sciences, Niigata University School of Medicine, Niigata 951-8518, Japan
[2]Graduate School of Science of Technology, Niigata University, Niigata 950-2181, Japan
[3]Department of Mechanical Engineering, Niigata University, Niigata 950-2181, Japan

(*Received 2 March 2009; received in revised form 14 May 2009; accepted 4 July 2009*)

Abstract
The purpose of the present study is to develop a direct and accurate method for measuring knee kinematics by using single-plane fluoroscopy. The 3-dimensional (3D) position of the bone (in other words, the 6 degree-of-freedom (DOF) parameters) was recovered by matching the digitally reconstructed radiographs (DRRs) generated from the 3D volume model of the bone on the basis of the fluoroscopic image. The root-mean-square error (RMSE) of the overall rotation parameters was within 2.1 degrees. For the translation parameters RMSE took its maximal value of 3.6 mm in the out-of-plane direction. This indicates that the present method has potential for clinical application.

Key words
Biomechanics, Knee Kinematics, Image Registration, Single-Plane Fluoroscopy, Orthopaedics

1. Introduction

Total knee arthroplasty is used for replacing deformed joints with implants in order to restore joint alignment and facilitate joint motion. Currently, the position in which the implant must be placed is determined by X-ray and/or computed tomography (CT) in a standing or supine position, which does not account for knee kinematics under dynamic weight-bearing conditions. This is due to the lack of knowledge regarding the kinematics of physiological and pathological knees.

Motion analysis systems using video cameras and skin-mounted markers have been widely used in the study of gross body motion. However, these systems capture large soft-tissue artefacts across the knee flexion angle when measuring the motion of the underlying bone [1]. Single-plane fluoroscopy has been used as a more direct method for measuring the kinematics of artificial knees [2-5]. Since the silhouette of a metallic implant is clearly observable in 2D fluoroscopic images, the 3D posture (full 6 degree-of-freedom (DOF) parameters) can be estimated by matching the calculated projection of the implant's 3D model with the silhouette. Several researchers have applied this technique to the measurement of natural knee motion [15-17]. However, the accuracy of their results was lower than that of studies applied to implanted knee joints due to less clear bone edges and imperfect 3D bone models.

The present study aims at developing a direct and accurate method for measuring knee kinematics by using single-plane fluoroscopy. Real-time visualization of digitally reconstructed radiographs (DRRs) was achieved by projecting a 3D bone volume model derived from CT data. Automated image-based matching was developed in order to estimate the full 6 DOF parameters representing the 3D relative position of the femur with respect to the tibia. The estimated position parameters were compared with the true values measured by using a 3D coordinated measuring machine.

2. Materials and Methods

2.1 True value of the relative position

The study was carried out on a human cadaver knee. Three spherical markers were bonded to the femur and the tibia. The femur and the tibia were fixed by using an external fixation device (Fig. 1). The central coordinates of the sphere markers were measured by using a 3D coordinate measuring machine (BH504, Mitutoyo, Japan) in order to define the absolute position of each bone. The relative position of the femur with respect to the tibia was derived from their absolute positions, and was used as the true value.

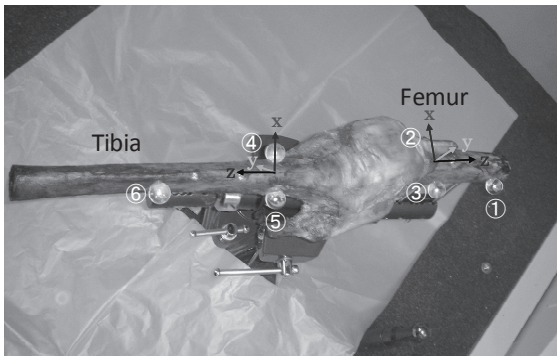

Fig. 1 Cadaver knee setup for measuring the true value of the relative position

2.2 DRR creation using bone volume models

Three-dimensional bone volume models were generated by bone segmentation of CT scan data of the femur and the tibia (field of view: 640 x 512 pixel, pixel size: 0.35 x 0.35 mm^2, slice thickness: 1 mm). The original anisotropic voxel, 0.35 x 0.35 x 1.0 mm^3, was transformed into an isotropic voxel with a volume of 1.0 x 1.0 x 1.0 mm^3 by using a 3D spline interpolation method in order to speed up the computation time and improve the quality of the DRR. The local coordinate system of the bone model was determined on the basis of the center coordinates of the markers as shown in Fig. 2. The DRR was created by projecting the all voxels onto the image plane. The pixel intensity is the cumulative attenuation of the projected voxel. The individual pixel intensity at a point (u,v) was calculated from the following equation

$$I(u,v) = I_0 e^{-\sum_{i=1}^{n} \alpha \mu_i} \quad (1)$$

where I_0 indicates the dynamic range, n is the number of voxels projected to the point (u,v), α is the attenuation factor, and μ_i is the voxel value. The values of I_0 and α were selected in such a way that the value of I matched that of the actual fluoroscopic image.

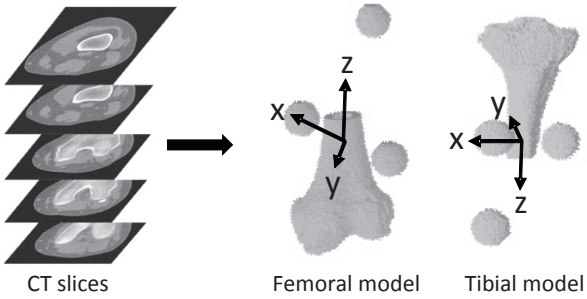

Fig. 2 Femoral and tibial volume models with their coordinate systems

2.3 Single-plane fluoroscopy

A single-plane fluoroscopic system (ADVANTEX E, GE Yokogawa Medical System, Japan) was used at a resolution of 1024 x 1024 pixels (covering an area of 320 mm x 320 mm) and an 8-bit gray scale depth. Using the grid pattern, the distortion of the fluoroscopic image was corrected by using a cubic polynomial equation [6] as shown in Fig. 3.

Camera calibration was performed on the corrected image by using a set of 40 spherical stainless markers embedded in an acrylic frame in order to determine the projection matrix. The projection matrix provides the 3D positions of the focal spot of the X-ray tube and the image plane with respect to the calibration frame in such a way that the projections of the bone volume model can be replicated in the image plane by the X-ray exposure. Fluoroscopic images of the cadaver knee were taken from 6 different directions (Fig. 4).

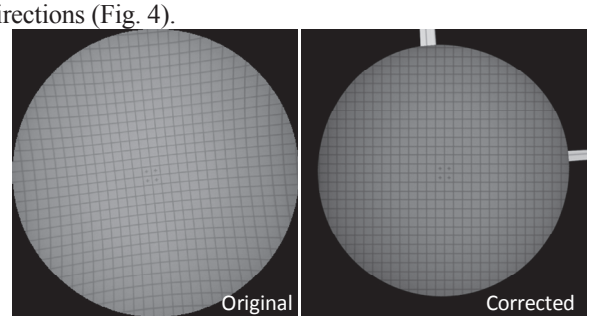

Fig. 3 Distortion correction of the fluoroscopic image

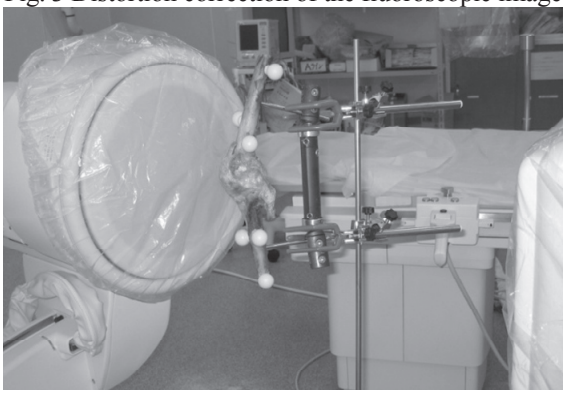

Fig. 4 Cadaver knee set up for the acquisition of a single-plane fluoroscopic image

2.4 Image-based matching procedure

In order to estimate the 6 DOF parameters of the bone, two measures which match in the fluoroscopic image and the DRR were assessed: one is the gradient difference in the pixel intensities defined as follows [7]

$$G(s)=\sum_{u,v}\frac{A_v}{A_v+(I_{diffV}(u,v))^2}+\sum_{u,v}\frac{A_h}{A_h+(I_{diffH}(u,v))^2} \tag{2}$$

$$\begin{cases} I_{diffV}(u,v)=\dfrac{dI_{fl}}{du}-s\dfrac{dI_{DRR}}{du} \\ I_{diffH}(u,v)=\dfrac{dI_{fl}}{dv}-s\dfrac{dI_{DRR}}{dv} \end{cases}$$

where I_{fl} and I_{DRR} are the intensities of the fluoroscopic image and the DRR, respectively. A_v and A_h denote the vertical and horizontal variances of the gradient in fluoroscopic image. The value of the scaling factor s is chosen to be between zero and unity in such a way that G takes its maximum value.

The other measure is the difference in contours of the bone image and the DRR. For the i-th point of the bone contour, $\mathbf{p}_i$, which is the closest point of the projected outline of the corresponding DRR, $\mathbf{q}_i$, was examined. The distance between the two points was summed over all bone contour points and was subsequently normalized by the total number of points, N.

$$D=\sum_{i=1}^{N}\frac{|\mathbf{p}_i-\mathbf{q}_i|}{N} \tag{3}$$

The overall matching measure is a simple summation of the two

$$F=-G+D \tag{4}$$

The 6 DOF parameters of the bone were determined by translation and rotation of the bone model until a minimum value of F was found by using a downhill simplex algorithm [8]. Note that since G is always positive, and the greater it becomes, the closer DRR becomes to the fluoroscopic image. Thus, the value of G was taken as negative for the purpose of minimization.

In this study, the contours of the femur and the tibia in the fluoroscopic images were detected by means of the Canny operator [9]. In order to compare the relative position of the femur with respect to the tibia by using the true value, the 6 DOF parameters of the tibia were first determined by performing manual image matching. Then, the femur was placed according to the true value of the relative position. Finally, an automated image matching algorithm was executed with respect to the femur. Figure 5 depicts the outline of the iterative process of the automated image matching process.

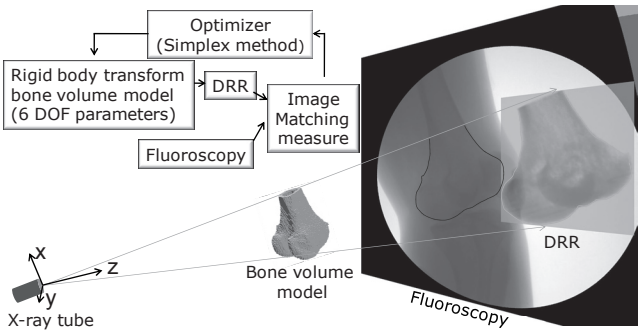

Fig. 5 Outline of the image matching procedure

3. Results

Figure 6 shows the DRRs of the femur and tibia matched to the fluoroscopic image. Note that the fibula and the patella were excluded from the image matching. The running time for minimization on a Windows® XP PC (XEON™ processor, 3 GHz, 3 GB RAM) was about 8 min for each bone.

The average error values, the standard deviations, and the root-mean-square errors [RMSEs] of the relative position parameters are listed in Table 1. The coordinate system is the same as the one set for the X-ray source, as shown in Fig. 5. The translation parameters were estimated within -0.3 mm ±1.0 mm for the x-axis, 0.8 mm ± 0.7 mm for the y-axis, and 2.2 mm ± 3.2 mm for the z-axis. The rotation parameters were estimated within 0.2 deg ± 2.3 deg for the x-axis, -0.5 deg ± 0.1 deg for the y-axis, and 0.6 deg ± 0.2 deg for the z-axis. The largest RMSEs were 3.6 mm at the translation along the z-axis and 2.1 deg at the rotation about the x-axis.

Figures 7 and 8 show an example of the changes in the matching measure F with the deviation of the translation and rotation parameters from their true values. For the in-plane (x and y) translations, the value of F decreased sharply as the deviation from the true value approached zero. However, for the out-of-plane (z) translation, it was almost constant around the true value. For all of the 3 rotation parameters, the shapes of the changes in F were very similar, regardless of the directions of their axes relative to the image plane. The bias was large in the rotation about the x-axis, resulting in the large RMSE listed in Table 1.

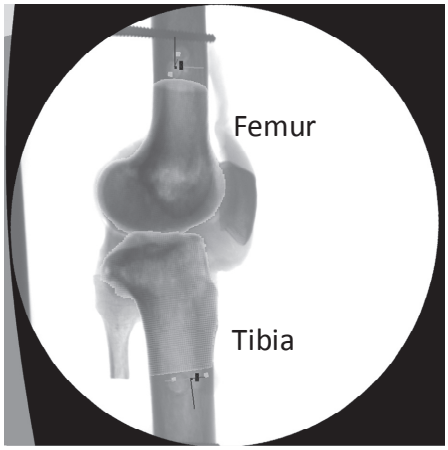

Fig. 6 Fluoroscopic image of a cadaver knee with its DRR overlaid

Table 1 Average error, standard deviation, and [RMSE] of estimating the rotation and translation parameters (n=6)

Translation (mm)		
x	y	z
-0.3±1.0 [1.0]	0.8±0.7 [1.0]	2.2±3.2 [3.6]

Rotation (deg)		
x	y	z
0.2±2.3 [2.1]	-0.5±0.1 [0.5]	0.6±0.2 [0.6]

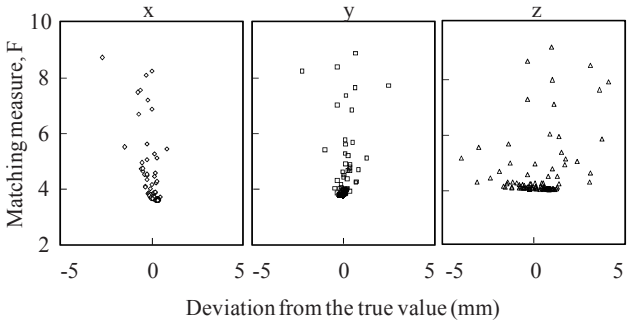

Fig. 7 Changes in F with the translation parameters

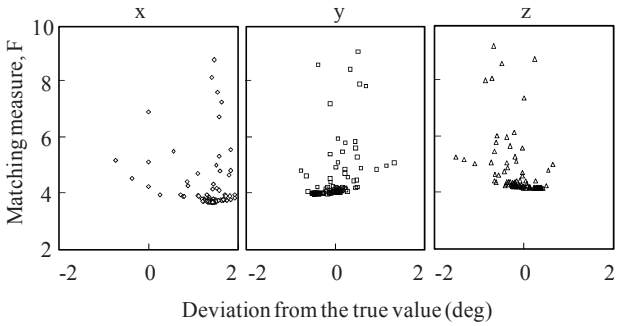

Fig. 8 Changes in F with the rotation parameters

4. Discussion

Direct 3D measurements of bone position have been investigated by using marker-based techniques [10,11] and image-based techniques [12-16]. Each of these techniques is based on bi-plane [10-14] or single-plane X-ray exposure [15-17]. The marker-based technique requires implanting radiopaque markers inside the bone. Although this procedure can be performed during surgery, such as total knee arthroplasty (TKA) or anterior cruciate ligament (ACL) reconstruction, the application of this technique to healthy subjects is severely restricted due to ethical reasons.

The image-based techniques represent a more practical approach since they do not require the insertion of any markers into bone. The precision of this technique using Roentgen stereophotogrammetric analysis (RSA) was reported to be 0.09 mm for the in-plane translation and 0.22 mm for the out-of-plane translation, and 0.24 deg for rotation about the out-of-plane axis and 0.07 deg about the in-plane axis when a sawbone scapula was used as a subject [12]. By using dual orthogonal fluoroscopic images, Li et al. [14] showed that the average error in measuring the distance

between the center of a ball and the surface of a cylinder was within 0.1 mm. The orientation of the cylinder was measured with an average accuracy of 0.1 deg.

Regarding single-plane radiography, Fregly et al. [15] investigated the theoretical accuracy of estimating the position under ideal conditions, where synthetic images were used to eliminate error sources such as blurred bone edges and image distortion. The precision was 0.20 mm for the in-plane translation and 3.1 mm for the out-of-plane translation, and 0.45 deg for the overall rotations. Other researchers used actual internal bone contours as well as bone edges. Their precision results were 0.45 mm [16] and 1.2 mm [17] for the in-plane translation, 4.0 mm [17] for the out-of-plane translation, and 0.66 deg [16] and 0.8 deg [17] for the overall rotations. These results were comparable to those of our study.

Ideally, the errors of our study can be regarded as negligible since the automated image matching started from the true value. However, several factors, such as the lowered clarity of the bone edge due to the surrounding soft tissue and the imperfect bone volume models, are contributing to the decrease of accuracy. In addition, similarly to previous studies, the inaccuracy of estimating the out-of-plane translation is still inevitable. As shown in Figs. 4 and 5, the reason for this inaccuracy is that the sensitivity of the matching measure to the changes in the out-of-plane translation is rather low. This can be explained in part by the magnifying ratio, which is determined on the basis of geometrical factors such as the pixel size, the focal distance, and the position of the subject. In our study, since the pixel size was 0.31 mm and the focal distance was 1100 mm, when a sphere with a diameter of 100 mm moves along the z-axis from a position at 600 mm to 602 mm, its projected edge shifts only 0.31 mm (equivalent to one pixel) on the image plane. Certainly, the closer the sphere to the X-ray tube, the larger the magnifying ratio. However, this also makes the penumbra larger. As shown in Fig. 9, the penumbra is introduced by the finite size of the focal spot of the X-ray tube and causes blurring of the edges and distortion in X-ray images [18]. Thus, sub-pixel image processing of bone edges might be effective for improving the sensitivity to changes in the out-of-plane translation.

Although single-plane fluoroscopy is less accurate than bi-plane fluoroscopy for the purpose of estimating the position of bones, it is more clinically feasible since it is available in many hospitals and has a larger viewing volume which allows subjects to perform a variety of motions. The application of this technique to measuring kneel, squat, and stair climb motions of normal knees has recently been reported [19]. Therefore, our method has a potential for the measurement of in vivo knee kinematics. Further research should be conducted to identify the sources of the errors in order to improve the reliability of the method and to examine the sensitivity to a given amount of change in each of the 6 DOF parameters.

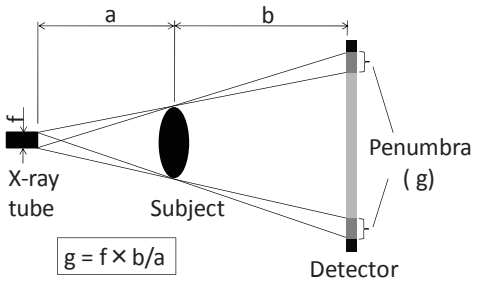

Fig. 9 Geometric factors producing the penumbra

5. Conclusions

A method for analyzing knee kinematics in vivo by using single-plane fluoroscopy and 3D bone models was developed. Digitally reconstructed radiographs (DRRs) were generated from 3D bone volume models with a voxel projection technique.

The relative 3D position (full 6 DOF parameters) of the femur and the tibia of a human cadaveric knee were determined by matching the DRR of each bone model with the fluoroscopic image by using an automated image-based matching technique with a downhill simplex algorithm.

The true value of the relative position was measured with a 3D coordinate measuring machine. The RMSE of the overall rotation parameters was within 2.1 degrees. Regarding the translation parameters, RMSE took its maximal value of 3.6 mm in the out-of-plane direction.

Nomenclature

a	distance from X-ray tube to subject
A_h, A_v	horizontal and vertical variances of the gradient in fluoroscopic image
b	distance from subject to detector
D	normalized difference between bone contour and projected outline of DRR
F	matching measure
f	focal size of X-ray tube
G	gradient difference
g	penumbra
I	pixel intensity
I_{diffh}	horizontal gradient difference
I_{diffv}	vertical gradient difference
I_{DRR}	pixel intensity of DRR
I_{fl}	pixel intensity of fluoroscopy
I_0	dynamic range of pixel intensity
N	the total number of bone contour
n	the number of voxels projected
$\mathbf{p}_i$	the i-th point of bone contour
$\mathbf{q}_i$	a point belongs to projected outline of the DRR and is closest to $\mathbf{p}_i$
s	scale factor
u,v	horizontal and vertical coordinates of the image plane
α	attenuation factor
μ	voxel value

Acknowledgement

This research was funded by a Grant-in-Aid for Scientific Research B No.19360046 provided by the Japan Society for the Promotion of Science.

References

[1] Garling, E.H., Kaptein, B.L., Mertens, B., Barendregt, W., Veeger, H.E.J., Nelissen, R.G.H.H. and Valster, E.R.: *J. Biomech.*, **40** (2007), S18-S24.

[2] Banks, S.A. and Hodge, W.A.: *IEEE Trans. Biomed. Eng.*, **43-6**(1996), 638-649.

[3] Zuffi, S., Leardini, A., Catani, F., Fantozzi, S. and Cappello, A.: *IEEE Trans. Med. Img.*, **18-10**(1999), 981-991.

[4] Mahfouz, M.R., Hoff, W.A., Komistek, R.D. and Dennis, D.A.: *IEEE Trans. Med. Img.*, **22-12**(2003), 1561-1574.

[5] Watanabe, T., Yamazaki, T., Sugamoto, K., Tomita, T., Hashimoto, H., Maeda, D., Tamura, S., Ochi, T. and Yoshikawa, H.: *J. Orthop. Res.*, 22(2004), 1044-1049.

[6] Haaker, P., Klotz, E., Koppe, R. and Linde, R.: Real-time distortion correction of digital X-ray II/TV-systems: an application example for digital flashing tomosynthesis (DFTS), *Int. J. Cardiac Imaging*, **6** (1990/91), 36-45.

[7] Penny, G.P., Weese, J., Little, J.A., Desmedt, P., Hill, D.L.G. and Hawkes, D.J.: *IEEE Trans. Med. Imging*, **17-4** (1998), 586-595.

[8] Nelder, J.A. and Mead, R.: A simplex method for function minimization, *Comp. J.,* **7**(1965), 308-13

[9] Canny, A.: *IEEE Trans. Pattr. Anal. Machine Intell.*, **8**(1986), 679-698

[10] Beardsley, C.L., Paller, D.J., Peura, G.D., Brattbakk, B. and Beynnon, B.D.: *J. Biomech.*, **40** (2007), 1417-1422.

[11] Tashman, S., Kolowich, P., Collon, D., Anderson, K. and Anderst, W.: *Clinical Orthop. Related Res*., **454** (2006), 66-73.

[12] de Bruin, P.W., Kaptein, B.L., Stoel, B.C. Reiber, J.H.C., Rozing, P.M. and Valstar, E.R.: Journal of Biomechanics, *J Biomech.*, **41** (2008), 155-164.

[13] You, B., Siy, P., Anderst, W. and Tashman, S.: *IEEE Trans. Med. Imging*, **20-6** (2001), 514-525.

[14] Li, G. Wuerz, T.H. and DeFrate, L.E.: *J. Biomech. Eng.*, **126** (2004), 314-318.

[15] Fregly, B.J., Rahman, H.A. and Banks, S.A.: *J. Biomech. Eng.*, **127** (2005), 692-99.

[16] Komistek, R.D., Dennis, D.A., and Mahfouz, M.R.: Clinical Orthopaedics and Related Research, *Clinical Orthop. Related Res*., **410** (2003), 69-81.

[17] Kanisawa, I., Banks, A.Z., Banks, S.A., Moriya, H. and Tsuchiya, A.: *Knee Surg. Sports Traumatol. Arthrosc***., 11** (2003), 16-22.

[18] Thornton, J.: *Eng. Failure Anal.*, **11** (2004), 207-220.

[19] Moro-oka, T., Hamai, S., Miura, H., Shimoto, T., Higaki, H., Fregly, G.J., Iwamoto, Y. and Banks, S.A.: *J. Orthop. Surg*., **26** (2007), 428-434.